

Electrolytes for Dye-Sensitized Solar Cells Based on Interhalogen Ionic Salts and Liquids

Mikhail Gorlov,[†] Henrik Pettersson,[‡] Anders Hagfeldt,[†] and Lars Kloo^{*†}*Center of Molecular Devices, Department of Chemistry, The Royal Institute of Technology, Teknikringen 30, S-100 44 Stockholm, Sweden, and IVF Industrial Research and Development Corporation, Argongatan 30, S-431 53 Mölndal, Sweden*

Received November 24, 2006

In this paper, we report on the preparation of interhalogen ionic liquids of the general formula $[K^+]XY_2^-$, where $K^+ = 1,3$ -dialkylimidazolium, 1,2,3-trialkylimidazolium, or *N*-alkylpyridinium; $XY_2^- = IBr_2^-$ or I_2Br^- . These compounds were characterized in solution and the solid state by NMR, IR, Raman, and mass spectroscopy. The crystal structure of the compound $[Me_2Bulm]IBr_2$ (**7**) shows that the IBr_2^- anion has a linear Br–I–Br structure. Indications of an equilibrium between different forms of XY_2^- anions in solution are observed. Interhalogen ionic salts and liquids were used as electrolyte components for encapsulated monolithic dye-sensitized solar cells. Overall light-to-electricity conversion efficiencies up to 6.4%, 5.0%, and 2.4% at 1000 W/m² were achieved by using electrolytes based on interhalogen ionic salts and γ -butyrolactone, glutaronitrile, or native ionic liquids as solvents, respectively. Moreover, in terms of stability, the cell performance lost 9–14% of the initial performance after 1000 h illumination at 350 W/m².

1. Introduction

Dye-sensitized nanostructured solar cells (DSCs), which were presented in 1991 by Grätzel, provide an alternative concept to the present p–n junction photovoltaic devices.¹ DSCs have been intensively investigated during the past decade because of their potential low cost of production and high-energy conversion efficiency.^{2–6} One concern for practical applications of DSCs is the use of electrolytes based on organic solvents. Attractive alternatives to organic solvents are nonvolatile, room-temperature ionic liquids. In addition, ionic liquids have favorable features such as chemical stability, relative nonflammability, and a wide electrochemical window.

Ionic liquids based on 1,3-dialkylimidazolium iodides have been widely used as solvents for DSCs.^{2–4,6} However, the relatively high viscosity of this type of imidazolium ionic liquids appears to limit their use because of transport limitations. In order to decrease viscosity, mixtures of ionic liquids containing different anions have successfully been tested.^{2,3} Ionic liquids based on alkyylimidazolium cations were also used as key components for quasisolid (gel) electrolytes.^{7–13} Different organic gelators^{7–11} or inorganic additives^{12,13} have been used in order to solidify alkyylimidazolium ionic liquids; overall light-to-electricity conversion efficiencies of about 6–7% have been achieved for certain quasisolid electrolytes.¹³

* To whom correspondence should be addressed. E-mail: Larsa@kth.se.

[†] The Royal Institute of Technology.[‡] IVF Industrial Research and Development Corporation.

- (1) Grätzel, M. *Nature* **2001**, *414*, 338.
- (2) Wang, P.; Zakeeruddin, S. M.; Moser, J.-E.; Grätzel, M. *J. Phys. Chem. B* **2003**, *107*, 13280.
- (3) Wang, P.; Zakeeruddin, S. M.; Humphry-Baker, R.; Grätzel, M. *Chem. Mater.* **2004**, *16*, 2694.
- (4) Otaka, H.; Kira, M.; Yano, K.; Ito, S.; Mitekura, H.; Kawata, T.; Matsui, F. *J. Photochem. Photobiol., A* **2004**, *164*, 67.
- (5) Xue, B.; Wang, H.; Hu, Y.; Li, H.; Wang, Z.; Meng, Q.; Huang, X.; Sato, O.; Chen, L.; Fujishima, A. *Photochem. Photobiol. Sci.* **2004**, *3*, 918.
- (6) Yamanaka, N.; Kawano, R.; Kubo, W.; Kitamura, T.; Wada, Y.; Watanabe, M.; Yanagida, S. *Chem. Commun.* **2005**, 740.

- (7) Kubo, W.; Kambe, S.; Nakade, S.; Kitamura, T.; Hanabusa, K.; Wada, Y.; Yanagida, S. *J. Phys. Chem. B* **2003**, *107*, 4374.
- (8) Kubo, W.; Kitamura, T.; Hanabusa, K.; Wada, Y.; Yanagida, S. *Chem. Commun.* **2002**, 374.
- (9) Wang, P.; Zakeeruddin, S. M.; Exnar, I.; Grätzel, M. *Chem. Commun.* **2002**, 2972.
- (10) Wang, P.; Zakeeruddin, S. M.; Moser, J. E.; Nazeeruddin, M. K.; Sekiguchi, T.; Grätzel, M. *Nat. Mater.* **2003**, *2*, 402.
- (11) Kim, Y. J.; Kim, J. H.; Kang, M.-S.; Lee, M. J.; Won, J.; Lee, J. C.; Kang, Y. S. *Adv. Mater.* **2004**, *16*, 1753.
- (12) Scully, S. R.; Lloyd, M. T.; Herrera, R.; Gannelis, E. P.; Malliaras, G. G. *Synth. Met.* **2004**, *144*, 291.
- (13) Wang, P.; Zakeeruddin, S. M.; Comte, P.; Exnar, I.; Grätzel, M. *J. Am. Chem. Soc.* **2003**, *125*, 1166.

Aside from 1,3-dialkylimidazolium ionic liquids, other types of molten salts have been tested as solvents for DSCs. Thus, it was found that trialkylsulfonium polyiodides exhibit good electrical conductivity.¹⁴ We have recently reported that DSCs with iodine-doped trialkylsulfonium iodides as electrolyte achieved an overall light-to-electricity conversion efficiency of 3.7% at a light intensity of 0.1 Sun (100 W/m²).¹⁵ Moreover, metal-iodide-doped trialkylsulfonium iodides have been investigated as electrolytes in DSCs; an overall light-to-electricity conversion efficiency of 3.1% (0.1 Sun) was achieved by using an electrolyte based on a (Bu₂-MeS)I:AgI:I₂ mixture.¹⁶

It is well-known that strong interaction between cations and anions in ionic liquids determines their physical properties, and in particular their viscosity. This fact was used for the preparation of nonviscous ionic liquids and their use as electrolytes for DSCs.^{2,3} The iodide/triiodide redox couple is commonly used in DSCs. The diffusion coefficient of the triiodide ion strongly depends on the viscosity of electrolyte. Hence, chemical modification of the anionic and/or cationic part of an ionic liquid can decrease its viscosity, with improved performance of the solar cells as result.

The chemistry of trihalide anions in solution and in the solid state has been widely studied for many years.^{17–20} The nature of bonding in trihalide anions has been analyzed.²¹ The crystal structures and vibrational spectroscopic data are obtained for salts containing organic as well as inorganic cations.^{22–26} The synthesis and properties of 1,3-dialkylimidazolium ionic liquids containing interhalogen anions such as IBr₂⁻, ICl₂⁻, etc. have recently been reported.^{27,28} These interhalogen ionic liquids (IILs) show much lower viscosity in comparison with the corresponding iodides; in some cases, the difference is a factor of 100–200.²⁸ This fact makes IILs

attractive as solvents or components of electrolytes for DSCs. There is also a possibility that lower optical absorption in the visible region of the spectrum may allow higher halogen concentrations, and thus, an extra enhancement of transport efficiency may be achieved. Also, interhalogen anions XY₂⁻ consisting of different halide atoms X and Y in conjunction with the corresponding halide ions X⁻ or Y⁻ can act as new redox couples with more efficiently adapted energy levels with respect to the sensitizing dye and counter electrode.

In the present work, we describe the preparation and characterization of new interhalogen ionic liquids, and their use as key components in electrolytes for dye-sensitized solar cells. Three types of electrolytes, based on glutaronitrile, γ -butyrolactone, or native ionic liquids as solvent, have been studied.

2. Experimental Section

2.1. Materials and Instrumentation. Glutaronitrile and γ -butyrolactone were distilled under reduced pressure before use. All other reagents and solvents were obtained from commercial sources and used as received. C, H, and N elemental analyses were carried out by Mikro Kemi AB (Uppsala, Sweden).

All quantum chemical calculations were performed using Gaussian03 (rev B.04).²⁹ Quasirelativistic effective core potentials were used for both Br (28 electrons) and I (46 electrons).³⁰ The valence spaces of the halogens were uncontracted of (5s5p1d) and (7s6p1d) quality for Br and I, respectively.^{30,31} Calculations were made using the hybrid functionals B3LYP and B3PW91, as well as perturbation theory using the second-order Møller–Plesset method. In order to investigate the polarizing effect of a dielectric solvent, the implemented version of the polarizable continuum model (PCM) based on the integral equation formalism was used for water ($\epsilon = 78.39$), acetonitrile ($\epsilon = 36.64$), and benzene ($\epsilon = 2.247$). The united atom model employing default radii was used to create the spherical cavities around all atoms in the interhalogen molecules studied.

Positive-ion FAB mass spectra were obtained on a Trio 2000 instrument by bombarding 3-nitrobenzyl alcohol matrices of the samples with 8 keV Xe atoms. Mass calibration for data system acquisition was achieved using CsI.

Electrospray ionization mass spectra were recorded on a Bruker esquire 3000 ion trap mass spectrometer, in both positive and negative ion modes, equipped with an orthogonal electrospray interface (Bruker Daltonics, Bremen, Germany). The Bruker

- (14) Stegemann, H.; Reiche, A.; Schnitke, A.; Fullbier, H. *Electrochim. Acta* **1992**, *37*, 379.
- (15) Paulsson, H.; Hagfeldt, A.; Kloo, L. *J. Phys. Chem. B* **2003**, *107*, 13665.
- (16) Paulsson, H.; Berggrund, M.; Svantesson, E.; Hagfeldt, A.; Kloo, L. *Sol. Energy Mater. Sol. Cells* **2004**, *82*, 345.
- (17) Popov, A. I. *Halogen Chemistry*; Gutmann, V., Ed.; Academic Press: New York, 1967; Vol. I, p 225.
- (18) Downs, A. J.; Adams, C. J. *Comprehensive Inorganic Chemistry*; Bailar, J. C., Emeleus, H. J., Nyholm, R. S., Trotman-Dickenson, A. F., Eds.; Pergamon: Oxford, 1973; Vol. II, p 1534.
- (19) Cotton, F. A.; Wilkinson, G.; Murillo, C. A.; Bochmann, M. *Advanced Inorganic Chemistry*, 6th ed.; John Wiley & Sons: New York, 1999; p 583.
- (20) Greenwood, N. N.; Earnshaw, A. *Chemistry of the Elements*, 2nd ed.; Pergamon: Oxford; p 835.
- (21) Landrum, G. A.; Goldberg, N.; Hoffmann, R. *J. Chem. Soc., Dalton Trans.* **1997**, 3605.
- (22) Domerq, B.; Devic, T.; Fourmigué, M.; Auban-Senzier, P.; Canadell, E. *J. Mater. Chem.* **2001**, *11*, 1570.
- (23) Murray, H. H., III; Porter, L. C.; Fackler, J. P., Jr.; Raptis, R. G. *J. Chem. Soc., Dalton Trans.* **1988**, 2669.
- (24) Naito, T.; Tateno, A.; Udagawa, T.; Kobayashi, H.; Kato, R.; Kobayashi, A.; Nogami, T. *J. Chem. Soc., Faraday Trans.* **1994**, *90*, 763.
- (25) Emge, T. J.; Wang, H. H.; Beno, M. A.; Leung, P. C. W.; Firestone, M. A.; Jenkins, H. C.; Cook, J. D.; Carlson, K. D.; Williams, J. M.; Venturini, E. L.; Azevedo, L. J.; Schirber, J. E. *Inorg. Chem.* **1985**, *24*, 1736.
- (26) Svensson, P. H.; Kloo, L. *J. Chem. Soc., Dalton Trans.* **2000**, 2449.
- (27) Bortolini, O.; Bottai, M.; Chiappe, C.; Conte, V.; Pieraccini, D. *Green Chem.* **2002**, *4*, 621.
- (28) Bagno, A.; Butts, C.; Chiappe, C.; D'Amico, F.; Lord, J. C. D.; Pieraccini, D.; Rastrelli, F. *Org. Biomol. Chem.* **2005**, *3*, 1624.

- (29) Frisch, M. J.; Trucks, G. W.; Schlegel, H. B.; Scuseria, G. E.; Robb, M. A.; Cheeseman, J. R.; Montgomery, J. A., Jr.; Vreven, T.; Kudin, K. N.; Burant, J. C.; Millam, J. M.; Iyengar, S. S.; Tomasi, J.; Barone, V.; Mennucci, B.; Cossi, M.; Scalmani, G.; Rega, N.; Petersson, G. A.; Nakatsuji, H.; Hada, M.; Ehara, M.; Toyota, K.; Fukuda, R.; Hasegawa, J.; Ishida, M.; Nakajima, T.; Honda, Y.; Kitao, O.; Nakai, H.; Klene, M.; Li, X.; Knox, J. E.; Hratchian, H. P.; Cross, J. B.; Bakken, V.; Adamo, C.; Jaramillo, J.; Gomperts, R.; Stratmann, R. E.; Yazyev, O.; Austin, A. J.; Cammi, R.; Pomelli, C.; Ochterski, J. W.; Ayala, P. Y.; Morokuma, K.; Voth, G. A.; Salvador, P.; Dannenberg, J. J.; Zakrzewski, V. G.; Dapprich, S.; Daniels, A. D.; Strain, M. C.; Farkas, O.; Malick, D. K.; Rabuck, A. D.; Raghavachari, K.; Foresman, J. B.; Ortiz, J. V.; Cui, Q.; Baboul, A. G.; Clifford, S.; Cioslowski, J.; Stefanov, B. B.; Liu, G.; Liashenko, A.; Piskorz, P.; Komaromi, I.; Martin, R. L.; Fox, D. J.; Keith, T.; Al-Laham, M. A.; Peng, C. Y.; Nanayakkara, A.; Challacombe, M.; Gill, P. M. W.; Johnson, B.; Chen, W.; Wong, M. W.; Gonzalez, C.; Pople, J. A. *Gaussian 03*, revision C.02; Gaussian, Inc.: Wallingford, CT, 2004.
- (30) Bergner, A.; Dolg, M.; Küchle, W.; Stoll, H.; Preuss, H. *Mol. Phys.* **1993**, *80*, 1431.
- (31) Schwerdtfeger, P.; Dolg, M.; Schwarz, W. H. E.; Bowmaker, G. A.; Boyd, P. D. W. *J. Chem. Phys.* **1989**, *91*, 1762.

Daltonics esquire 5.2 (Build 382) software bundle consisting of Bruker esquire Control 5.2 (Build 63.8) and Bruker Data Analysis 3.2 (Build 121) were used for acquiring spectra and data analysis, respectively. The samples were delivered at a flow rate of 4 $\mu\text{L}/\text{min}$ using a syringe pump 74900 from Cole-Parmer Instrument Company (Vernon Hills, IL), and N_2 was used as drying and nebulizing gas (flow rates 5 L/min).

Raman spectra were recorded with a Bio-Rad FTS 6000 spectrometer equipped with a low-power Nd:YAG laser ($\lambda = 1064$ nm) and a liquid-nitrogen-cooled, solid-state Ge diode detector. A resolution of 4 cm^{-1} was used. Typical laser power at the samples was 500–800 mW.

IR spectra were recorded with a Bio-Rad FT-375C spectrometer using NaCl plates for neat liquids or chloroform solutions.

^1H and ^{13}C NMR spectra were obtained on a Bruker DMX 500 spectrometer. The spectra were recorded at 298 K in CDCl_3 solution using TMS as external reference.

Diffraction data were collected on a Bruker-Nonius KappaCCD diffractometer. Numerical absorption corrections were applied.³² The structure was solved using direct methods³³ and refined on R^2 with anisotropic thermal parameters for all non-H atoms.³⁴ H atoms were refined on calculated positions using a riding model. CCDC-605792 contains the supplementary crystallographic data. These data can be obtained free of charge from the Cambridge Crystallographic Data Centre via www.ccdc.cam.ac.uk/data_request/cif.

Electrochemical experiments (cyclic voltammetry and conductivity measurements) were performed using a CHI-660 electrochemical work station. Cyclic voltammetry and differential pulse voltammetry were recorded in acetonitrile (concentration of IILs was 1.25 mM) under nitrogen atmosphere. Scan rate was 0.5 V/s for **12** and 0.1 V/s for **7** and $[\text{HexPy}]_3$. Supporting electrolyte ($n\text{-C}_4\text{H}_9$)₄NPF₆ in acetonitrile (50 mM), Pt foil as counter electrode, Ag/Ag⁺ as reference electrode were all used.

The diffusion constants $D(\text{A}^-)$ of I_3^- , IBr_2^- , and I_2Br^- were determined by measuring the limiting current density J_{lim} , according to the following equation³⁵

$$J_{\text{lim}} = 2nqD(\text{A}^-)c(\text{A}^-)N_{\text{A}}/d$$

where n is the number of electrons, q is the elemental charge, $c(\text{A}^-)$ is the concentration of I_3^- , IBr_2^- , or I_2Br^- , and N_{A} is Avogadro's constant. Cyclic voltammetry was performed to measure J_{lim} using a two-electrode cell consisting of two platinized conducting glass electrodes separated at a fixed distance d (40 μm) and connected to a potentiostat.

The overall light-to-electricity conversion efficiency (η), fill factor (FF), open-circuit voltage (V_{oc}), and short-circuit current density (J_{sc}) were obtained through the current–voltage characteristics of a solar cell at room temperature. These were monitored and recorded using a computerized Keithley model 2400 source unit. A microwave-powered sulfur plasma lamp, Light Drive 1000,

was used as source of illumination. The lamp was calibrated versus the solar spectrum, and the efficiencies correspond to the AM 1.5 spectrum.

2.2. Synthesis of Interhalogen Ionic Liquids. General Procedures for Preparation of 1–14. The starting materials, alkylimidazolium or alkylpyridinium iodides or bromides, were prepared by the reaction of 1-methylimidazole, 1,2-dimethylimidazole, or pyridine with alkyl iodides or alkyl bromides in tetrahydrofuran (boiling for 3 h with following washing with tetrahydrofuran and drying under dynamic vacuum). Corresponding alkylimidazolium or alkylpyridinium iodide (10 mmol) was dissolved in chloroform (10 mL), and the solution was cooled to 5 $^{\circ}\text{C}$ (ice bath). An equimolar amount of Br_2 or IBr was dissolved in chloroform (5 mL), and the solution was added drop-by-drop to the solution of alkylimidazolium or alkylpyridinium iodide under stirring. The temperature of the mixture was kept in the interval 5–10 $^{\circ}\text{C}$ during the whole reaction time. The color of the solution turned from transparent to dark brown when the first drops of Br_2 or IBr solution were added (probably because of formation of iodine), but in the end of the reaction it became orange-red, and two phases formed. The upper layer was removed, and the remaining red-orange oil was heated at 50 $^{\circ}\text{C}$ for 1 h under reduced pressure. The yield was 80–95%.

1-Methyl-3-ethylimidazolium Iododibromide, 1. Red liquid. IR (liquid film): 3143 (vs), 3108 (vs), 2980 (m), 2949 (w), 1568 (vs), 1462 (s), 1446 (s), 1385 (w), 1336 (w), 1165 (vs), 1087 (w), 1026 (w), 958 (w), 829 (s), 743 (s), 700 (w), 642 (m), 619 (s) cm^{-1} . ESI-MS: $m/z = 111$ [MeEtIm^+], 287 [IBr_2^-], 334 [I_2Br^-]. ^1H NMR (CDCl_3 , 500 MHz): δ 1.62 (t, CH_3), 4.05 (s, N-CH_3), 4.35 (q, N-CH_2), 7.14 (d, CH), 7.31 (d, CH), 9.08 (s, CH) ppm. ^{13}C NMR (CDCl_3 , 500 MHz): δ 15.5 (s, CH_3), 15.8 (s, CH_3), 37.5 (s, CH_2), 45.9 (s, CH_3), 46.1 (s, CH_3), 122.1 (s, CH), 122.4 (s, CH), 123.8 (s, CH), 123.9 (s, CH), 136.3 (s, NCN), 136.4 (s, NCN) ppm.

1-Methyl-3-propylimidazolium Iododibromide, 2. Red liquid. IR (liquid film): 3142 (vs), 3105 (vs), 2965 (vs), 2876 (m), 1568 (vs), 1456 (s), 1426 (m), 1340 (w), 1166 (vs), 1088 (w), 1018 (w), 902 (w), 829 (s), 799 (w), 748 (s), 647 (m), 620 (s) cm^{-1} . ESI-MS: $m/z = 125$ [MePrIm^+], 288 [IBr_2^-], 334 [I_2Br^-], 381 [I_3^-]. ^1H NMR (CDCl_3 , 500 MHz): δ 0.99 (t, CH_3), 1.96 (sextet, CH_2), 4.06 (s, N-CH_3), 4.23 (t, N-CH_2), 7.34 (d, CH), 9.30 (s, CH) ppm. ^{13}C NMR (CDCl_3 , 500 MHz): δ 11.0 (d, CH_3), 23.7 (d, CH_2), 37.4 (d, CH_2), 52.2 (s, CH_3), 122.4 (s, CH), 123.8 (s, CH), 136.7 (s, NCN) ppm.

1-Methyl-3-hexylimidazolium Iododibromide, 3. Red liquid. IR (liquid film): 3141 (s), 3107 (s), 2954 (vs), 2930 (vs), 2857 (s), 1566 (s), 1561 (s), 1464 (s), 1457 (s), 1377 (w), 1338 (w), 1164 (vs), 1104 (w), 829 (m), 742 (m), 648 (w), 619 (s) cm^{-1} . Anal. Calcd for $\text{C}_{10}\text{H}_{19}\text{N}_2\text{IBr}_2$: C, 26.45; H, 4.19; N, 6.17. Found: C, 26.8; H, 4.4; N, 6.3. FAB⁺-MS: $m/z = 167$ [HexMeIm^+]. ^1H NMR (CDCl_3 , 500 MHz): 0.83 (t, CH_3), 1.28 (br, $(\text{CH}_2)_2$), 1.34 (br s, CH_2), 1.90 (quintet, CH_2), 4.04 (s, N-CH_3), 4.23 (t, N-CH_2), 7.33 (s, CH), 7.36 (s, CH), 8.89 (s, CH) ppm. ^{13}C NMR (CDCl_3 , 500 MHz): δ 14.0 (s, CH_3), 22.4 (s, CH_2), 26.0 (s, CH_2), 30.2 (s, CH_2), 31.0 (s, CH_2), 37.6 (s, CH_2), 50.9 (s, CH_3), 122.6 (s, CH), 124.0 (s, CH), 136.1 (s, NCN) ppm.

1-Methyl-3-hexylimidazolium Bromodiiodide, 4. Red liquid. IR (liquid film): 3139 (s), 3103 (s), 2952 (vs), 2928 (vs), 2856 (s), 1568 (s), 1561 (s), 1464 (s), 1457 (s), 1376 (w), 1338 (w), 1163 (vs), 1104 (w), 1021 (w), 826 (m), 740 (m), 648 (w), 618 (s) cm^{-1} . ESI-MS: $m/z = 167$ [MeHexIm^+]. ^1H NMR (CDCl_3 , 500 MHz): 0.83 (t, CH_3), 1.28 (br, $(\text{CH}_2)_2$), 1.35 (br, CH_2), 1.91 (quintet, CH_2), 4.05 (s, N-CH_3), 4.25 (t, N-CH_2), 7.33 (s, CH), 7.36 (s,

- (32) A red crystal of **7** was selected for X-ray structural analysis on a Bruker-Nonius KappaCCD diffractometer at 299 K. The compound crystallized in the space group $P2_1/c$, monoclinic, $a = 15.2999(10)$ \AA , $b = 7.7057(5)$ \AA , $c = 13.4781(5)$ \AA , $\beta = 111.123(4)^\circ$, $V = 1482.25(15)$ \AA^3 , $Z = 4$, $\rho_{\text{calcd}} = 1.972$ $\text{g}\cdot\text{cm}^{-3}$, Mo $\text{K}\alpha$ radiation, $\lambda = 0.71073$ \AA . Final R values: $R1 = 0.0651$, $wR2 = 0.1519$; GOF = 1.156 for 2572 unique reflections and 130 parameters. Herrendorf, W.; Bärnighausen H.: *HABITUS, a program for numerical absorption correction*; Universities of Giessen and Karlsruhe: Germany, 1997.
- (33) Sheldrick, G. S. *SHELXS97, a program for crystal structure solution*; University of Göttingen: Göttingen, Germany, 1997.
- (34) Sheldrick, G. S. *SHELXL97, a program for crystal structure refinement*; University of Göttingen: Göttingen, Germany, 1997.
- (35) Hauch, A.; Georg, A. *Electrochim. Acta* **2001**, *46*, 3457.

CH), 9.01 (s, CH) ppm. ^{13}C NMR (CDCl_3 , 500 MHz): δ 14.0 (s, CH_3), 22.4 (s, CH_2), 26.0 (s, CH_2), 30.2 (s, CH_2), 31.1 (s, CH_2), 37.8 (s, CH_2), 51.0 (s, CH_3), 122.6 (s, CH), 124.0 (s, CH), 136.3 (s, NCN) ppm.

1-Methyl-3-dodecylimidazolium Iododibromide, 5. Yellow solid. IR (liquid film, solution in CHCl_3): 2993 (s), 2927 (vs), 2855 (s), 1587 (w), 1568 (m), 1462 (m), 1426 (w), 1378 (w), 1164 (s), 822 (w), 620 (m) cm^{-1} . ESI-MS: $m/z = 251$ [MeDodIm^+], 286.7 [IBr_2^-], 334.2 [I_2Br^-]. ^1H NMR (CDCl_3 , 500 MHz): 0.80 (t, CH_3), 1.18 (br, $(\text{CH}_2)_7$), 1.31 (br, $(\text{CH}_2)_2$), 1.90 (quintet, CH_2), 4.05 (s, $\text{N}-\text{CH}_3$), 4.22 (t, $\text{N}-\text{CH}_2$), 7.32 (s, CH), 7.35 (s, CH), 8.85 (s, CH) ppm. ^{13}C NMR (CDCl_3 , 500 MHz): δ 14.1 (s, CH_3), 22.6 (s, CH_2), 26.4 (s, CH_2), 29.0 (s, CH_2), 29.3 (s, CH_2), 29.4 (s, CH_2), 29.5 (s, CH_2), 29.6 (s, CH_2), 30.2 (s, CH_2), 31.9 (s, CH_2), 37.7 (s, CH_2), 51.0 (s, CH_3), 122.6 (s, CH), 124.0 (s, CH), 136.2 (s, NCN) ppm.

1-Methyl-3-propylimidazolium Tribromide, 6. Red liquid. IR (liquid film): 3143 (vs), 3108 (vs), 2965 (vs), 2935 (w), 2876 (m), 1566 (vs), 1457 (s), 1387 (w), 1339 (w), 1165 (vs), 1104 (w), 1088 (w), 832 (s), 746 (s), 647 (m), 620 (s) cm^{-1} . ESI-MS: $m/z = 125.2$ [MePrIm^+]. ^1H NMR (CDCl_3 , 500 MHz): δ 0.70 (t, CH_3), 0.99 (t, CH_3), 1.69 (sextet, CH_2), 1.96 (sextet, CH_2), 3.77 (s, $\text{N}-\text{CH}_3$), 3.97 (t, $\text{N}-\text{CH}_2$), 4.05 (s, $\text{N}-\text{CH}_3$), 4.24 (t, $\text{N}-\text{CH}_2$), 7.22 (d, CH), 7.32 (d, CH), 8.57 (s, CH), 9.05 (s, CH) ppm. ^{13}C NMR (CDCl_3 , 500 MHz): δ 10.9 (d, CH_3), 23.6 (s, CH_2), 23.7 (s, CH_2), 37.3 (s, CH_2), 37.4 (s, CH_2), 51.9 (s, CH_3), 52.2 (s, CH_3), 122.3 (s, CH), 122.6 (s, CH), 123.7 (s, CH), 123.9 (s, CH), 135.6 (s, NCN), 136.5 (s, NCN) ppm.

1,2-Dimethyl-3-butylimidazolium Iododibromide, 7. Dark red solid. IR (liquid film, solution in CHCl_3): 3134 (s), 2989 (s), 2961 (vs), 2933 (s), 2872 (m), 1587 (s), 1535 (s), 1463 (s), 1459 (s), 1418 (m), 1381 (m), 1340 (w), 1232 (s), 1183 (w), 1132 (m), 1037 (w), 626 (w) cm^{-1} . Anal. Calcd for $\text{C}_9\text{H}_{17}\text{N}_2\text{IBr}_2$: C, 24.56; H, 3.87; N, 6.37. Found: C, 25.5; H, 3.9; N, 6.5. FAB $^+$ -MS: $m/z = 153$ [Me_2BuIm^+]. ^1H NMR (CDCl_3 , 500 MHz): δ 0.89 (t, CH_3), 1.33 (sextet, CH_2), 1.77 (q, CH_2), 2.67 (s, $\text{C}_{\text{ring}}-\text{CH}_3$), 3.85 (s, $\text{N}-\text{CH}_3$), 4.06 (t, $\text{N}-\text{CH}_2$), 7.25 (s, CH), 7.30 (s, CH) ppm. ^{13}C NMR (CDCl_3 , 500 MHz): δ 11.0 (s, CH_3), 13.7 (s, CH_2), 19.8 (s, CH_2), 31.7 (s, CH_2), 36.5 (s, CH_3), 49.2 (s, CH_3), 121.2 (s, CH), 122.9 (s, CH), 143.6 (s, NCN) ppm.

1,2-Dimethyl-3-butylimidazolium Bromodiiodide, 8. Dark red liquid. IR (liquid film): 3133 (s), 2957 (vs), 2931 (vs), 2868 (s), 1585 (vs), 1558 (w), 1535 (vs), 1458 (vs), 1418 (m), 1379 (m), 1340 (w), 1268 (w), 1244 (s), 1183 (w), 1132 (s), 1075 (w), 1036 (w), 741 (vs), 662 (s), 625 (w) cm^{-1} . ESI-MS: $m/z = 153.1$ [Me_2BuIm^+]. ^1H NMR (CDCl_3 , 500 MHz): δ 0.94 (t, CH_3), 1.39 (sextet, CH_2), 1.82 (q, CH_2), 2.73 (s, $\text{C}_{\text{ring}}-\text{CH}_3$), 3.89 (s, $\text{N}-\text{CH}_3$), 4.10 (t, $\text{N}-\text{CH}_2$), 7.24 (d, CH), 7.29 (d, CH) ppm. ^{13}C NMR (CDCl_3 , 500 MHz): δ 11.4 (s, CH_3), 13.6 (s, CH_2), 19.8 (s, CH_2), 31.7 (s, CH_2), 36.8 (s, CH_3), 49.4 (s, CH_3), 121.3 (s, CH), 123.0 (s, CH), 143.7 (s, NCN) ppm.

1,2-Dimethyl-3-hexylimidazolium Iododibromide, 9. Dark red liquid. IR (liquid film): 3133 (s), 2954 (vs), 2928 (vs), 2857 (s), 1585 (s), 1535 (s), 1464 (s), 1458(s), 1418 (m), 1378 (m), 1339 (w), 1268 (w), 1240 (s), 1171 (w), 1132 (m), 1105 (w), 1078 (w), 1036 (w), 743 (s), 662 (s), 626 (w) cm^{-1} . ESI-MS: $m/z = 181$ [$\text{Me}_2\text{HexIm}^+$], 288.2 [IBr_2^-], 334.6 [I_2Br^-]. ^1H NMR (CDCl_3 , 500 MHz): δ 0.83 (t, CH_3), 1.27 ($(\text{CH}_2)_2$), 1.32 (CH_2), 1.81 (q, CH_2), 2.70 (s, $\text{C}_{\text{ring}}-\text{CH}_3$), 3.87 (s, $\text{N}-\text{CH}_3$), 4.07 (t, $\text{N}-\text{CH}_2$), 7.21 (d, CH), 7.25 (d, CH) ppm. ^{13}C NMR (CDCl_3 , 500 MHz): δ 11.0 (s, CH_3), 14.0 (s, CH_2), 22.4 (s, CH_2), 26.3 (s, CH_2), 29.7 (s, CH_2), 31.1 (s, CH_2), 36.5 (s, CH_3), 49.5 (s, CH_3), 121.2 (s, CH), 122.9 (s, CH), 143.7 (s, NCN) ppm.

1,2-Dimethyl-3-octylimidazolium Bromodiiodide, 10. Dark red liquid. IR (liquid film): 3133 (s), 2952 (vs), 2925 (vs), 2854 (s), 1585 (s), 1559 (w), 1535 (s), 1464 (s), 1458(s), 1418 (m), 1378 (m), 1340 (w), 1278 (w), 1238 (s), 1163 (w), 1132 (m), 1106 (w), 1080 (w), 1036 (w), 746 (s), 662 (s), 626 (w) cm^{-1} . ESI-MS: $m/z = 209$ [$\text{Me}_2\text{OctIm}^+$], 334.4 [I_2Br^-]. ^1H NMR (CDCl_3 , 500 MHz): δ 0.82 (t, CH_3), 1.21 ($(\text{CH}_2)_2$), 1.31 ($(\text{CH}_2)_3$), 1.83 (q, CH_2), 2.73 (s, $\text{C}_{\text{ring}}-\text{CH}_3$), 3.89 (s, $\text{N}-\text{CH}_3$), 4.09 (t, $\text{N}-\text{CH}_2$), 7.22 (d, CH), 7.27 (d, CH) ppm. ^{13}C NMR (CDCl_3 , 500 MHz): δ 11.3 (s, CH_3), 14.1 (s, CH_2), 22.6 (s, CH_2), 26.5 (s, CH_2), 28.9 (s, CH_2), 29.0 (s, CH_2), 29.8 (s, CH_2), 31.7 (s, CH_2), 36.8 (s, CH_3), 49.7 (s, CH_3), 121.2 (s, CH), 123.0 (s, CH), 143.6 (s, NCN) ppm.

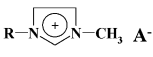
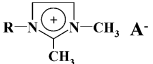
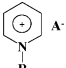
1,2-Dimethyl-3-dodecylimidazolium Iododibromide, 11. Orange-red solid. IR (liquid film, solution in CHCl_3): 3134 (s), 2990 (m), 2925 (vs), 2854 (s), 1583 (m), 1558 (w), 1534 (m), 1465 (m), 1458 (m), 1419 (w), 1377 (w), 1339 (w), 1236 (w), 1133 (w), 626 (w) cm^{-1} . ESI-MS: $m/z = 265.0$ [$\text{Me}_2\text{DodIm}^+$], 287.7 [IBr_2^-], 334.0 [I_2Br^-]. ^1H NMR (CDCl_3 , 500 MHz): δ 0.80 (t, CH_3), 1.19 ($(\text{CH}_2)_7$), 1.30 ($(\text{CH}_2)_2$), 1.81 (q, CH_2), 2.70 (s, $\text{C}_{\text{ring}}-\text{CH}_3$), 3.88 (s, $\text{N}-\text{CH}_3$), 4.07 (t, $\text{N}-\text{CH}_2$), 7.20 (d, CH), 7.25 (d, CH) ppm. ^{13}C NMR (CDCl_3 , 500 MHz): δ 11.0 (s, CH_3), 14.1 (s, CH_2), 22.6 (s, CH_2), 26.5 (s, CH_2), 29.0 (s, CH_2), 29.3 (s, CH_2), 29.4 (s, CH_2), 29.5 (s, CH_2), 29.6 (s, CH_2), 29.7 (s, CH_2), 31.7 (s, CH_2), 36.5 (s, CH_3), 49.5 (s, CH_3), 121.2 (s, CH), 122.9 (s, CH), 143.7 (s, NCN) ppm.

N-Butylpyridinium Iododibromide, 12. Dark red liquid. IR (liquid film): 3124 (w), 3055(s), 2960 (s), 2932 (s), 2868 (m), 1631 (vs), 1498 (s), 1485 (vs), 1464 (s), 1376 (w), 1317 (w), 1212 (w), 1171 (s), 1056 (w), 950 (w), 766 (s), 733 (w), 680 (vs) cm^{-1} . Anal. Calcd for $\text{C}_9\text{H}_{14}\text{N}_2\text{IBr}_2$: C, 25.55; H, 3.31; N, 3.31. Found: C, 26.8; H, 3.6; N, 3.4. FAB $^+$ -MS: $m/z = 136$ [BuPy^+]. ^1H NMR (CDCl_3 , 500 MHz): δ 0.65 (t, CH_3), 0.96 (t, CH_3), 1.13 (sextet, CH_2), 1.44 (sextet, CH_2), 1.76 (q, CH_2), 2.04 (q, CH_2), 4.43 (t, $\text{N}-\text{CH}_2$), 4.77 (t, $\text{N}-\text{CH}_2$), 7.86 (t, CH), 8.13 (t, CH), 8.32 (t, CH), 8.52 (t, CH), 8.71 (d, CH), 9.01 (d, CH) ppm. ^{13}C NMR (CDCl_3 , 500 MHz): δ 13.6 (s, CH_3), 13.7 (s, CH_3), 19.5 (s, CH_2), 19.6 (s, CH_2), 33.5 (s, CH_2), 33.7 (s, CH_2), 62.4 (s, CH_2), 62.9 (s, CH_2), 128.9 (s, CH), 129.0 (s, CH), 144.3 (s, CH), 144.6 (s, CH), 145.6 (s, CH), 145.8 (s, CH). The deviation of experimental values in elemental analysis data is due to negligible impurities which are difficult to remove by distillation or recrystallization.

N-Butylpyridinium Bromodiiodide, 13. Dark red liquid. IR (liquid film): 3123 (w), 3055 (s), 2959 (s), 2931 (s), 2868 (m), 1632 (vs), 1498 (s), 1485 (vs), 1458 (s), 1376 (w), 1315 (w), 1211 (w), 1169 (s), 1055 (w), 949 (w), 765 (s), 733 (w), 679 (vs) cm^{-1} . ESI-MS: $m/z = 136.1$ [BuPy^+], 334.6 [I_2Br^-], 380.3 [I_2BuPy^-]. ^1H NMR (CDCl_3 , 500 MHz): δ 0.98 (t, CH_3), 1.44 (sextet, CH_2), 2.07 (q, CH_2), 4.75 (t, $\text{N}-\text{CH}_2$), 8.13 (t, CH), 8.53 (t, CH), 8.93 (d, CH) ppm. ^{13}C NMR (CDCl_3 , 500 MHz): δ 11.6 (s, CH_3), 19.6 (s, CH_2), 33.6 (s, CH_2), 63.2 (s, CH_2), 129.1 (s, CH), 144.6 (t, CH), 145.6 (s, CH).

N-Dodecylpyridinium Iododibromide, 14. Orange-red solid. IR (liquid film, solution in CHCl_3): 3126 (w), 3058 (m), 2990 (s), 2926 (vs), 2854 (s), 1631 (s), 1499 (m), 1486 (s), 1462 (m), 1373 (w), 1316 (w), 1171 (s), 677 (s) cm^{-1} . ESI-MS: $m/z = 248.0$ [DodPy^+], 334.1 [I_2Br^-], 407.7 [$\text{Br}_2\text{DodPy}^-$]. ^1H NMR (CDCl_3 , 500 MHz): δ 0.80 (t, CH_3), 1.18 ($(\text{CH}_2)_7$), 1.34 ($(\text{CH}_2)_2$), 2.05 (q, CH_2), 4.69 (t, $\text{N}-\text{CH}_2$), 8.13 (t, CH), 8.54 (t, CH), 8.90 (d, CH) ppm. ^{13}C NMR (CDCl_3 , 500 MHz): δ 14.1 (s, CH_3), 22.6 (s, CH_2), 26.2 (s, CH_2), 29.0 (s, CH_2), 29.3 (s, CH_2), 29.5 (s, CH_2), 29.6 (s, CH_2), 31.8 (s, CH_2), 31.9 (s, CH_2), 63.2 (s, CH_2), 94.4 (t, CH_2), 129.1 (s, CH), 144.5 (t, CH), 145.8 (s, CH).

Table 1. Synthesized Interhalogen Ionic Salts and Liquids

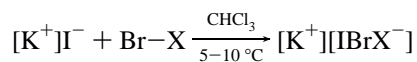
					
R	A ⁻	R	A ⁻	R	A ⁻
1	C ₂ H ₅	7	C ₄ H ₉	12	C ₄ H ₉
2	C ₃ H ₇	8	C ₄ H ₉	13	C ₄ H ₉
3	C ₆ H ₁₃	9	C ₆ H ₁₃	14	C ₁₂ H ₂₅
4	C ₆ H ₁₃	10	C ₈ H ₁₇		
5	C ₁₂ H ₂₅	11	C ₁₂ H ₂₅		
6	C ₃ H ₇				

3. Results and Discussion

3.1 Synthesis and Characterization of Ionic Liquids.

In this work, three types of interhalogen ionic liquids were studied: 1,3-dialkylimidazolium, 1,2,3-trialkylimidazolium, and *N*-alkylpyridinium salts. These aromatic cations were chosen because of their high electrochemical stability and relatively low viscosity of the ionic liquids in comparison with other types of ionic liquids, based, for example, on tetraalkylphosphonium cations. The counterions were IBr₂⁻ and I₂Br⁻. Compounds with different alkyl chains were prepared; the length of alkyl chain varied from -C₂H₅ to -C₁₂H₂₅.

The synthetic approach for the preparation of interhalogen ionic liquids was based on the reaction between alkylimidazolium or alkylpyridinium iodides and free bromine or iodine monobromide in chloroform solution



where K⁺ = 1,3-dialkylimidazolium, 1,2,3-trialkylimidazolium, or *N*-alkylpyridinium; X = Br or I.

Earlier, this method was used for the preparation of a series of IILs, but the reaction was carried out without any solvent.^{27,28} We used mild reaction conditions (low temperature and gradual addition of Br₂ or IBr) in order to avoid halogenation of the organic cations. A series of ionic liquids was prepared on the basis of this reaction, see Table 1.

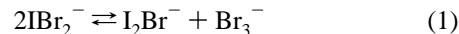
Compounds **1–4**, **6**, **8–10**, **12**, and **13** are red liquids, immiscible with water and quite soluble in acetone. Salt **5** is a yellow solid, **7** is a dark red solid, and **11** and **14** are orange-red solids. The yields of IILs were typically high (80–95%). The melting points are 39 (**5**), 37 (**7**), 47 (**11**), and 37 (**14**) °C.

In order to confirm the structure of the cationic part of the IILs, the compounds were characterized by ¹H and ¹³C NMR spectroscopy in CDCl₃ solution. In comparison with the corresponding iodides, the IILs have almost identical ¹H NMR spectra (Supporting Information). It is interesting to note that ¹H and ¹³C NMR spectra of **1**, **6**, and **12** contain double sets of the peaks. This probably may be explained by the presence of free cations K⁺ and ion pair, such as (K⁺)-(IBr₂⁻), in chloroform solution.

Several IILs prepared are solid at room temperature. This gave us the possibility to use single-crystal X-ray diffraction analysis in order to confirm the structure of the compounds in crystalline form. It was particularly important to determine the structure of the interhalogen anions. The compound [Me₂-

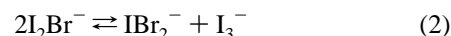
BuIm]IBr₂ (**7**) was characterized by single-crystal X-ray diffraction analysis.^{32–34} The molecular and crystal structures are shown in Figure 1. The compound consists of planar imidazolium rings and linear IBr₂⁻ anions. It is important to note that the iodine atom occupies the central position and is surrounded by two bromine atoms. The I–Br distance is 2.7085(11) Å, which is slightly shorter than the calculated value for the linear [Br–I–Br]⁻ anion (2.766 Å; B3PW91). Another essential characteristic of this compound is the absence of significant interaction between the IBr₂⁻ anion and the Me₂BuIm⁺ cation in the crystal structure; the shortest distance between Br or I atoms and H atoms is 3.1 Å. Commonly, ionic liquids show a network of hydrogen bonds (see, for example, refs 37 and 38). One can assume that the absence of strong cation–anion interaction accounts for the relatively low viscosity of interhalogen ionic liquids.

Mass spectroscopy (fast atom bombardment and electro-spray ionization spectroscopy) was also used for characterization of the compounds prepared. All spectra are shown in the Supporting Information. Methanol solutions (concentration 0.1 mg/mL) were used. Positive ion mode spectra of all compounds contain single peaks corresponding to alkylimidazolium or alkylpyridinium cations. It is important to note that the negative ion mode spectra of all ionic liquids with IBr₂⁻ anions contain peaks with *m/z* = 286.7 [IBr₂⁻] and *m/z* = 334.7 [I₂Br⁻]. This fact may be explained by the existence of an equilibrium between different anions in solution:



The ratio of intensities of peaks corresponding to [IBr₂⁻] and [BrI₂⁻] anions depends on the nature of the cation and may reflect the interaction between cations and anions in solution. For compounds **7** and **12**, the ratio [IBr₂⁻]:[BrI₂⁻] is about 2:1, which indicates that a significant amount of [IBr₂⁻] anions is transformed into other forms.

Negative ion mode spectrum of the [Me₂BuIm]I₂Br (**8**) ionic liquid contains three peaks: *m/z* = 380.6 [I₃⁻], *m/z* = 334.7 [BrI₂⁻], and *m/z* = 286.7 [IBr₂⁻], which can be explained by the existence of an equilibrium in solution:



It should be noted that similar behavior of potassium salts containing interhalogen anions I₂Cl⁻ and I₂Br⁻ was observed in aqueous and acetonitrile solutions.³⁹ Thus, on the basis of mass spectrometric results, the authors postulate the existence of equilibria such as those in eqs 1 and 2.³⁹ The absence of some peaks in negative mode mass spectra, for

(36) Pettersson, H.; Gruszecki, T.; Bernhard, R.; Häggman, L.; Gorlov, M.; Boschloo, G.; Edvinsson, T.; Kloo, L.; Hagfeldt, A. *Prog. Photovolt: Res. Appl.*, in press.

(37) Anderson, J. L.; Ding, R.; Ellern, A.; Armstrong, D. W. *J. Am. Chem. Soc.* **2005**, *127*, 593.

(38) Vygodskii, Y. S.; Lozinskaya, E. I.; Shaplov, A. S.; Lyssenko, K. A.; Antipin, M. Yu.; Urman, Y. G. *Polymer* **2004**, *45*, 5031.

(39) McIndoe, J. S.; Tuck, D. J. *Dalton Trans.* **2003**, 244.

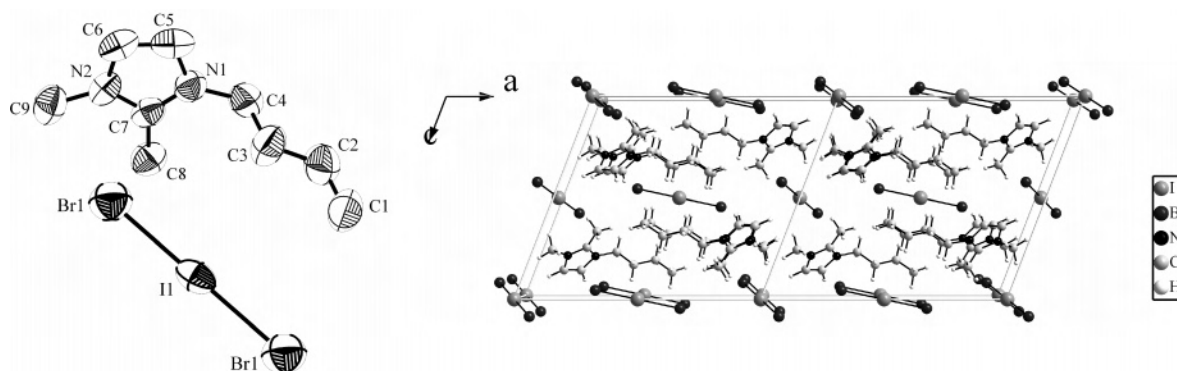


Figure 1. Molecular (with thermal ellipsoids at 50% probability) and crystal structure of $[\text{Me}_2\text{BuIm}]\text{IBr}_2$ (**7**). Selected bond distances (\AA) and angles (deg): $\text{Br1}-\text{I1} = 2.7085(11)$, $\text{N1}-\text{C5} = 1.376(11)$, $\text{C6}-\text{C5} = 1.316(13)$, $\text{N2}-\text{C6} = 1.360(11)$, $\text{N2}-\text{C7} = 1.317(10)$, $\text{N1}-\text{C7} = 1.324(10)$, $\text{Br1}-\text{I1}-\text{Br1} = 180(0)$.

Table 2. Bands in Raman Spectra of Interhalogens in the Ionic Liquids

compd	expt	band, cm^{-1}			ion	symm	
		calcd					
		B3PW91	B3LYP	MP2			
$[\text{Me}_2\text{BuIm}]\text{IBr}_2$ (7) ^a	157.2 (s); 132.8 (m)						
$[\text{Me}_2\text{HexIm}]\text{IBr}_2$ (9) ^a	158.5 (s)						
$[\text{Me}_2\text{C}_{12}\text{H}_{25}\text{Im}]\text{IBr}_2$ (11) ^a	157.6 (s)						
$[\text{HexMeIm}]\text{IBr}_2$ (3) ^a	153.6 (s)						
$[\text{PrMeIm}]\text{IBr}_2$ (2) ^a	158.1 (s); 134.5 (m)	151	144	158	$[\text{Br}-\text{I}-\text{Br}]^-$	$D_{\infty h}$	
$[\text{EtMeIm}]\text{IBr}_2$ (1) ^a	158.7 (s)	132; 179	125; 170	137; 198	$[\text{Br}-\text{Br}-\text{I}]^-$	$C_{\infty v}$	
$[\text{BuPy}]\text{IBr}_2$ (12) ^a	157.2 (s); 136.5 (m)						
$[\text{C}_{12}\text{H}_{25}\text{Py}]\text{IBr}_2$ (14) ^a	155.6 (s)						
$[\text{MeC}_{12}\text{H}_{25}\text{Im}]\text{IBr}_2$ (5) ^a	159.8 (s)						
$[\text{Me}_2\text{OctIm}]\text{I}_2\text{Br}$ (10) ^b	157.8 (s); 133.4 (s); 111.8 (s)						
$[\text{Me}_2\text{BuIm}]\text{I}_2\text{Br}$ (8) ^a	153.9 (s); 132.3 (s); 110.9 (s)	125; 163	118; 154	130; 170	$[\text{I}-\text{I}-\text{Br}]^-$	$C_{\infty v}$	
$[\text{BuPy}]\text{I}_2\text{Br}$ (13) ^a	157.2 (s); 132.4 (s); 110.8 (s)	113	107	116	$[\text{I}-\text{Br}-\text{I}]^-$	$D_{\infty h}$	
$[\text{HexMeIm}]\text{I}_2\text{Br}$ (4) ^a	157.6 (s); 132.4 (s); 111.0 (s)						
Br_3^-	$[\text{PrMeIm}]\text{Br}_3$ (6) ^b	159.5 (s)	158	151	166	$[\text{Br}-\text{Br}-\text{Br}]^-$	$D_{\infty h}$
I_3^-			109	103	113	$[\text{I}-\text{I}-\text{I}]^-$	$D_{\infty h}$

^a In CHCl_3 . ^b Without solvent.

example Br_3^- peaks, may be explained by the formation of adducts between cations K^+ and anions, such as $[\text{KBr}_n]^-$. Indeed, negative ion mode spectrum of $[\text{Me}_2\text{HexIm}]\text{IBr}_2$ (**9**) contains a peak at $m/z = 341.7$ which corresponds to $[\text{Me}_2\text{HexImBr}_2]^-$ anion.

Quantum chemical calculations were performed in order to evaluate the thermodynamic stability of different anions coexisting in solution of interhalogen ionic liquids.²⁹ Calculations of changes of Gibbs free energy for reactions 1 and 2 at the B3PW91 level give the following results ($T = 298.150 \text{ K}$): $\Delta G^\circ = +33.2 \text{ kJ/mol}$ for eq 1 and $\Delta G^\circ = +2.5 \text{ kJ/mol}$ for eq 2. These correspond to equilibrium constants of $K_1 = 1.53 \times 10^{-6}$ and $K_2 = 0.36$. The inclusion of solvent effects using the PCM formalism for water, acetonitrile, and benzene, representing a wide scan in dielectric properties, did not significantly shift the change in Gibbs free energy of reactions 1 and 2 ($< 2 \text{ kJ mol}^{-1}$). The main reason is most likely that all molecular species in these two reactions with respect to topology and charge distribution are very similar. The experimental and calculational results allow us to conclude that (1) the nature of, in particular, the organic cation can play an important role with respect to shifts of equilibria; (2) several forms of anions can coexist in solution.

In order to confirm the presence of IBr_2^- or I_2Br^- anions

in solution, Raman spectra for IILs were recorded. Also, quantum chemical calculations were performed in order to assign the low-frequency bands in the Raman spectra.²⁹ Experimental and calculated frequency data for ionic liquids formally containing IBr_2^- , I_2Br^- , and Br_3^- anions are presented in Table 2. It should here be emphasized that although the composition of IILs implies the presence of XY_2^- anions, it is not necessary that these nominal ions dominate in the liquid state (see mass spectrometry data). One can state that predominance of XY_2^- anions is a starting hypothesis in the interpretation of vibrational spectroscopic data with the help of quantum chemical calculations.

Strong bands in region $153\text{--}159 \text{ cm}^{-1}$ are observed in Raman spectra of ionic liquids containing IBr_2^- anions in chloroform solutions. This is in good agreement with quantum chemical calculations showing one band at 151 cm^{-1} (B3PW91 level) for the $\text{Br}-\text{I}-\text{Br}^-$ anion ($D_{\infty h}$). Asymmetry of these bands can be explained by interaction between cations and anions in solution as well as the existence of vibrational excitations. The presence of Br_3^- anion in solution due to equilibria 1 and 2 can also be responsible for the asymmetry of these bands. According to the calculations, the second possible isomer, $[\text{Br}-\text{Br}-\text{I}]^-$, has its strongest Raman band at 132 cm^{-1} . One can assume

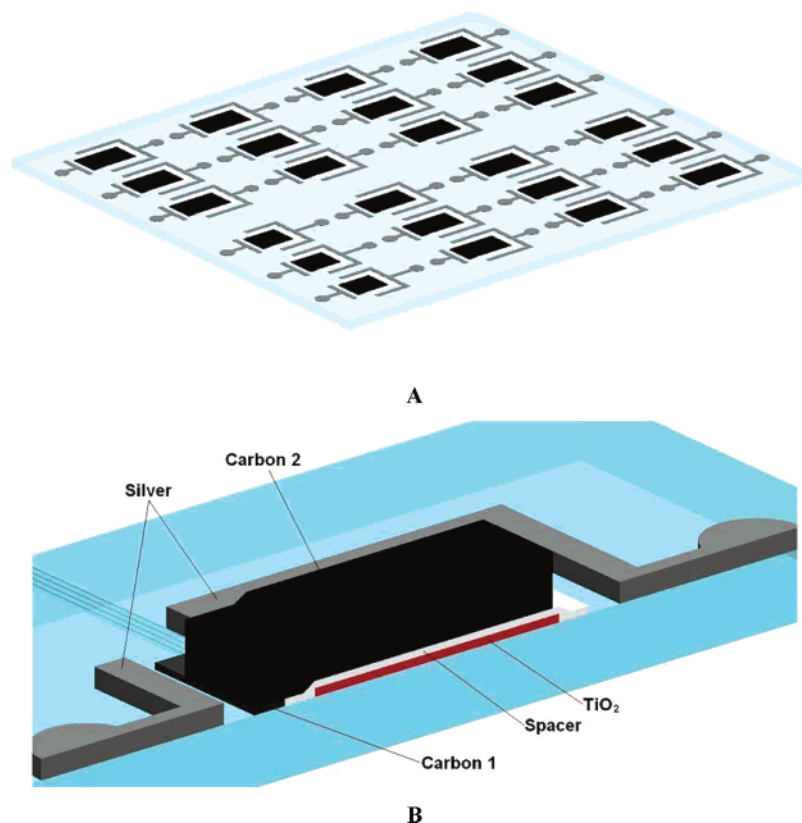


Figure 2. A monolithic multicell with 24 individual cells (A) and schematic cross-section of the four-layer monolithic dye-sensitized photovoltaic cell (B).

that the presence of an additional, less intense band in the region $132\text{--}136\text{ cm}^{-1}$ in the Raman spectra of certain IILs (Table 2) may be attributed to the presence of a second isomer in solution.

Raman spectra of IILs containing I_2Br^- anions contain three strong bands centered at 155 , 132 , and 110 cm^{-1} . The presence of these bands may be explained by the coexistence of the two isomers, $[\text{I}-\text{I}-\text{Br}]^-$ and $[\text{I}-\text{Br}-\text{I}]^-$, ions in solution. A strong band at 110 cm^{-1} may also originate from I_3^- in the liquid. It should be noted that our results are in good agreement with experimental and theoretical data recently obtained for series of organic salts with interhalogen anions.⁴⁰

In order to understand the electrochemical processes of IBr_2^- anions, it is necessary to compare them with those of the well-known iodide/triiodide redox couple I_3^-/I^- . According to literature data, the I_3^-/I^- couple is characterized by two oxidation processes in solution: $\text{I}^- \rightarrow \text{I}_3^-$ and $\text{I}_3^- \rightarrow \text{I}_2$.⁴¹ These data are in agreement with electrochemical behavior of alkylpyridinium and trialkylimidazolium triiodides. As an example, compound $[\text{HexPy}]_3\text{I}_3$ displays two oxidation processes in acetonitrile solution at $+0.887$ and 0.321 V versus NHE (cyclic voltammograms and differential pulse voltammetry results in Supporting Information). The electrochemical behavior of IILs was studied in acetonitrile solution using Ag/Ag^+ reference electrode under nitrogen

atmosphere. Compounds $[\text{Me}_2\text{BuIm}]\text{IBr}_2$ (**7**) and $[\text{BuPy}]\text{IBr}_2$ (**12**) display three oxidation steps at 1.22 , 0.75 , and 0.56 V versus NHE for **7**, and at 1.10 , 0.84 , and 0.60 V for **12** versus NHE (Supporting Information). It should be noted that IILs decompose under electrochemical reduction: small drops formed on the surface of acetonitrile solution at negative potentials, which causes the quality of voltammograms. Interhalogen anions IBr_2^- could in principle be oxidized to give products with higher nuclearity. Compounds with I_3Br_4^- anions are known, although only in the solid state.^{40,42} Taking that into account, and the fact that, according to Raman and mass spectra, IILs are present in solution in at least two isomers, makes it difficult to draw conclusions about the exact chemical composition of the oxidation products of IBr_2^- anions.

3.2. Solar Cell Performance. The solar cells used in this work were encapsulated four-layer monolithic multicells. A multicell means that several individual cells are manufactured on the same substrate in parallel processes allowing a high reproducibility of the cell performance. The multicell substrate contains 24 individual monolithic dye-sensitized solar cells with an active TiO_2 surface of 0.48 cm^2 (Figure 2A). Each monolithic cell consists of four layers: dye-sensitized TiO_2 layer, porous ZrO_2 layer (spacer), adhesion layer (carbon 1), and platinumized carbon layer (carbon 2). As can be seen in Figure 2B, the carbon 1 layer is placed next to the spacer layer whereas the carbon 2 layer is placed on top of the spacer layer and the carbon 1 layer. The thicknesses of the layers were approximately $12\text{ }\mu\text{m}$ (TiO_2),

(40) Aragoni, M. C.; Arca, M.; Devillanova, F. A.; Hursthouse, M. B.; Huth, S. L.; Isaia, F.; Lippolis, V.; Mancini, A.; Ogilvie, H. R.; Verani, G. *J. Organomet. Chem.* **2005**, *690*, 1923.

(41) Oskam, G.; Bergeron, B. V.; Meyer, G. J.; Searson, P. C. *J. Phys. Chem. B* **2001**, *105*, 6867.

(42) Minkwitz, R.; Berkei, M.; Ludwig, R. *Inorg. Chem.* **2001**, *40*, 25.

10 μm (spacer), 10 μm (carbon 1), and 50 μm (carbon 2). Details of the multicell manufacturing have been described in a separate work.³⁶ In short, the manufacturing technique is based on screen-printing the electrodes onto laser-structured transparent conducting glass (TEC 15 Ω/square from Hartford Glass). After sintering the electrodes, the glass plates are immersed in the dye solution. For the results presented in this paper, *cis*-di(thiocyanato)-bis(4,4'-dicarboxy-2,2'-bipyridine)Ru(II), in a concentration of 0.3 mM, dissolved in acetonitrile/*tert*-butanol (50/50 by volume), was used. The electrolyte solution is manually dispensed on the monolithic electrodes. Finally, the cells are sealed tightly in a vacuum-heat process using the encapsulation material Surlyn.

The following IILs were chosen as components of the electrolytes for monolithic DSCs: [PrMeIm]IBr₂ (**2**), [HexMeIm]IBr₂ (**3**), [HexMeIm]I₂Br (**4**), [Me₂Bulm]IBr₂ (**7**), and [BuPy]IBr₂ (**12**).

Three types of electrolytes have been studied in this work: (1) glutaronitrile as solvent, (2) γ -butyrolactone as solvent, and (3) the native ionic liquids as solvent. The composition of electrolytes, diffusion constants, and results of *IV*-measurements are shown in Table 3. It is important to note that, according to the Raman spectra of electrolytes, interhalogen anions are present in the solutions even in the presence of excess of iodide ions.

On the basis of analysis of the results presented in Table 3, the following conclusions can be made.

1. Overall, light-to-electricity conversion efficiencies of the cells with electrolytes based on ionic liquids as solvents are lower than those for glutaronitrile- or γ -butyrolactone-based electrolytes. For example, the difference between efficiencies of the pairs **E6–E9** and **E7–E11** is 2–3% in efficiency both at light intensities of 1000 and 100 W/m². This can be attributed to the higher viscosity of imidazolium ionic liquids in comparison to glutaronitrile solutions, which leads to slower ion transport in electrolyte (according to literature,²⁸ viscosity of [BuMeIm]I is 1110 cP and viscosity of [BuMeIm]IBr₂ is 57 cP). This is in agreement with lower values of diffusion constants for the ionic liquid electrolytes. It should be highlighted that the multicells have not yet been optimized for low-viscous electrolytes. The performance of cells using electrolytes **E9** and **E11** would benefit from the use of a more porous TiO₂ layer and a thinner spacer layer.

2. Overall light-to-electricity conversion efficiencies of the cells with electrolytes based on γ -butyrolactone are higher than those for glutaronitrile-based electrolytes mainly due to higher short-circuit current density values. The difference is 1.3–1.9% at light intensities of 1000 W/m² (the **E2–E13**, **E4–E14**, **E7–E15** pairs). Probably, this may be attributed to the lower viscosity of γ -butyrolactone compared with that for glutaronitrile (1.63 and 5.67 cP at 28 °C, respectively).⁴³

3. Glutaronitrile and γ -butyrolactone electrolytes contain two additives, guanidinium thiocyanate and 1-*N*-methylbenzimidazole. *N*-donor organic additives based on benzimidazole are frequently used as components of electrolytes

for DSCs.^{9,13,44} A comparison of efficiencies of these electrolytes with the corresponding ones without additives (the **E1–E2**, **E3–E4**, **E5–E6** pairs) shows that the former ones are more efficient (the difference is up to 0.9% in efficiency at 1000 W/m²) due to an increase in open-circuit photovoltage, as observed earlier.⁴⁴ Guanidinium thiocyanate may be adsorbed along with dye molecules at the TiO₂ surface, thus playing the role of a blocking layer and/or facilitating self-assembly agent, as considered by Grätzel.⁴⁵

4. The performance of the monolithic cells with electrolytes **E9** and **E10**, containing imidazolium ionic liquids with IBr₂[−] and I₂Br[−] anions, respectively, is very similar, which can be explained by the presence of similar redox-active species in solution due to the equilibria previously discussed in this work.

5. The influence of alkyl chain length in imidazolium cations on the performance of the monolithic cells was also studied (electrolytes **E6–E8**). The efficiency of the cells containing a short alkyl chain (C₃H₇) in imidazolium cations is slightly higher than the one for the cells containing longer alkyl chains (C₆H₁₃ and C₁₂H₂₅) at a light intensity of 1000 W/m². However, at a light intensity of 100 W/m², the difference is insignificant.

6. A comparison of glutaronitrile electrolytes containing the interhalogen anions IBr₂[−] or I₂Br[−] with glutaronitrile electrolyte containing the I₃[−] anion (**E12**) shows that the latter one is more efficient (the difference is 0.5–1% in efficiency at 1000 W/m²). It should be emphasized here that (1) the concentration of additives and combination between materials for electrodes were optimized for I[−]/I₃[−] electrolytes; (2) the performance of cells containing I[−]/I₃[−] redox couple loses 10% of the initial performance after 1000 h illumination at 350 W/m² (see ref 36); (3) in the case of I[−]/IBr₂[−] or I[−]/I₂Br[−] systems it is difficult to estimate which redox couple(s) work in real cell due to equilibria between different anions in solution.

Typical *IV*-characteristics of DSCs based on the interhalogen ionic liquids are displayed in Figure 3 (glutaronitrile or ionic liquid as solvent).

3.3. Stability of Monolithic Solar Cells with IILs Electrolytes. The long-term stability of the dye-sensitized solar cells is one of the most important characteristics for their practical application. In order to evaluate the stability under illumination of the monolithic solar cells containing IILs, three cells with electrolytes **E2**, **E4**, and **E6** were illuminated for 1000 h (6 weeks) at 350 W/m² using a sodium lamp (open-circuit condition) protected by a UV cutoff filter (cut off at 400 nm). Results from these experiments are shown in Figure 4.

The efficiencies of all cells decrease slowly during illumination. The relative decrease in efficiency after 6 weeks of illumination is 9% for electrolytes **E2** and **E6** and 14.5% for **E4**.

(44) Kusama, H.; Arakawa, H. *J. Photochem. Photobiol. A: Chem.* **2004**, *162*, 441.

(45) Grätzel, M. *J. Photochem. Photobiol. A: Chem.* **2004**, *164*, 3.

(43) Phibbs, M. K. *J. Phys. Chem.* **1955**, *59*, 346.

Table 3. Diffusion Constants D of IB_2^- , I_2Br^- , and I_3^- and Results Obtained from IV -Measurements of Monolithic Dye-Sensitized Multicells Based on Interhalogen Ionic Liquids^a

	composition	D (cm ² /s)	1000 W/m ²				100 W/m ²			
			η (%)	FF (%)	V_{oc} (V)	J_{sc} (mA/cm ²)	η (%)	FF (%)	V_{oc} (V)	J_{sc} (mA/cm ²)
E1	0.8 M [Me ₂ BuIm]I 0.1 M [BuMe ₂ Im]IBr ₂ in glutaronitrile	1.1×10^{-6}	4.1	59	0.72	9.6	4.8	66	0.66	1.1
E2	0.8 M [Me ₂ BuIm]I 0.1 M [BuMe ₂ Im]IBr ₂ 0.1 M GuanSCN ^b 0.5 M NMBI ^c in glutaronitrile	8.6×10^{-7}	4.9	61	0.77	10.2	6.0	72	0.73	1.1
E3	0.8 M [BuPy]I 0.1 M [BuPy]IBr ₂ in glutaronitrile	1.2×10^{-6}	4.1	59	0.70	9.8	4.2	69	0.62	1.0
E4	0.8 M [BuPy]I 0.1 M [BuPy]IBr ₂ 0.1 M GuanSCN 0.5 M NMBI in glutaronitrile	1.1×10^{-6}	4.5	58	0.74	10.3	6.0	71	0.69	1.2
E5	0.8 M HexMeImI 0.1 M [HexMeIm][IBr ₂] in glutaronitrile	1.3×10^{-6}	3.6	57	0.70	8.9	4.6	70	0.64	1.0
E6	0.8 M [HexMeIm]I 0.1 M [HexMeIm]IBr ₂ 0.1 M GuanSCN 0.5 M NMBI in glutaronitrile	— ^d	4.5	60	0.77	9.9	5.8	70	0.70	1.2
E7	0.8 M [PrMeIm]I 0.1 M [PrMeIm]IBr ₂ 0.1 M GuanSCN 0.5 M NMBI in glutaronitrile	1.9×10^{-6}	5.0	59	0.74	11.5	6.0	71	0.68	1.2
E8	0.8 M [C ₁₂ H ₂₅ MeIm]I 0.1 M [C ₁₂ H ₂₅ MeIm]IBr ₂ 0.1 M GuanSCN 0.5 M NMBI in glutaronitrile	1.4×10^{-6}	4.5	54	0.71	11.5	6.1	73	0.66	1.3
E9	0.1 M [HexMeIm]IBr ₂ 0.1 M GuanSCN 0.5 M NMBI in [HexMeIm]I	3.1×10^{-7}	2.3	43	0.62	8.6	3.2	56	0.56	1.0
E10	0.1 M [HexMeIm]I ₂ Br 0.1 M GuanSCN 0.5 M NMBI in [HexMeIm]I	3.2×10^{-7}	2.4	41	0.64	9.2	3.4	54	0.58	1.1
E11	0.1 M [PrMeIm]IBr ₂ 0.1 M GuanSCN 0.5 M NMBI in [PrMeIm]I	3.1×10^{-7}	2.3	48	0.63	7.6	3.0	61	0.56	0.9
E12	0.8 M [BuMeIm]I 50 mM I ₂ 0.1 M GuanSCN 0.2 M NMBI in glutaronitrile	1.5×10^{-6}	5.4	62	0.72	12.1	6.2	72	0.67	1.3
E13	0.8 M [Me ₂ BuIm]I 0.1 M [Me ₂ BuIm]IBr ₂ 0.1 M GuanSCN 0.5 M NMBI in γ -butyrolactone	— ^d	6.3	61	0.79	12.9	7.0	74	0.73	1.3
E14	0.8 M [BuPy]I 0.1 M [BuPy]IBr ₂ 0.1 M GuanSCN 0.5 M NMBI in γ -butyrolactone	— ^d	6.4	64	0.79	12.8	7.0	74	0.73	1.3
E15	0.8 M [PrMeIm]I 0.1 M [PrMeIm]IBr ₂ 0.1 M GuanSCN 0.5 M NMBI in γ -butyrolactone	— ^d	6.3	61	0.80	13.2	7.3	73	0.75	1.3

^a η = overall light-to-electricity conversion efficiency; FF = fill factor; V_{oc} = open-circuit voltage; J_{sc} = short-circuit current density. ^b GuanSCN = guanidinium thiocyanate. ^c NMBI = 1-*N*-methylbenzimidazole. ^d Limiting current density cannot be measured accurately because of the absence of well-defined plateau in cyclic voltammograms.

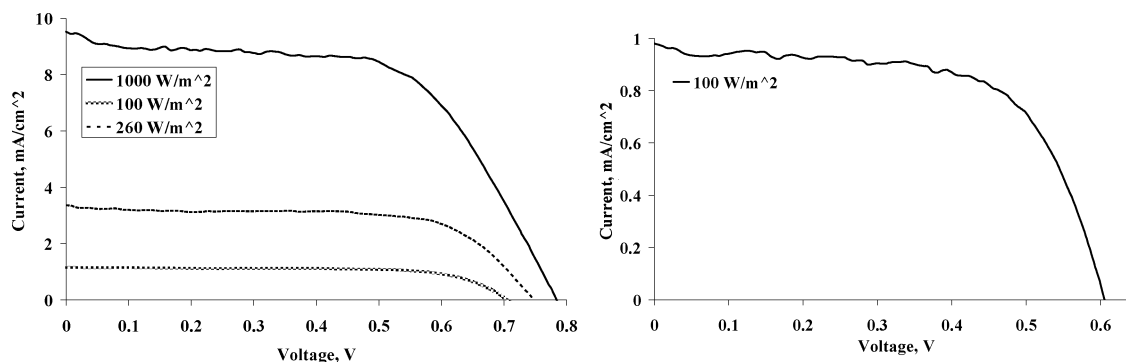


Figure 3. IV-characteristics of monolithic dye-sensitized multicells based on glutaronitrile electrolyte **E6** (left) and ionic liquid electrolyte **E9** (right). Both electrolytes **E6** and **E9** contain [HexMeIm]I and [HexMeIm]IBr₂ (**3**).

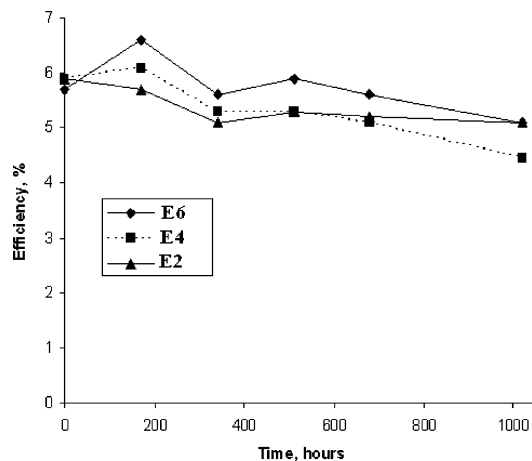


Figure 4. Efficiency changes with time for the cells with electrolytes **E2**, **E4**, and **E6** under illumination at 350 W/m².

4. Conclusions

New interhalogen ionic liquids have been prepared and characterized in solution and in the solid state. Ionic liquids containing IBr₂⁻ and I₂Br⁻ anions were successfully used as electrolyte components for monolithic dye-sensitized solar multicells. Overall light-to-electricity conversion efficiencies up to 6.4%, 5.0%, and 2.4% at 1000W/m² were achieved by using electrolytes based on interhalogen ionic salts and γ -butyrolactone, glutaronitrile, or native ionic liquids as solvents, respectively. The long-term stability under il-

lumination showed 9–14% relative efficiency degradation after 1000 h of illumination at 350 W/m². In conclusion, it was shown that a new type of low-viscous interhalogen ionic liquids containing a mixture of redox species provides promising alternatives to viscous ionic liquids based on alkylimidazolium iodides. In comparison with the classical I⁻/I₃⁻ redox system, interhalogen I⁻/IBr₂⁻ or I⁻/I₂Br⁻ redox couples are potentially more “flexible” redox species due to equilibria between different anions in solution. In order to achieve higher efficiency and improved long-term stability of electrolytes based on interhalogen ionic liquids, optimization of all components of DSCs (semiconductor materials, dyes, sealing materials) will be required. The use of new organic dyes and different sealing materials in conjunction with interhalogen ionic liquid electrolytes is currently under investigation in our group.

Acknowledgment. We thank Dr. A. Nazarov (Institut für Anorganische Chemie, Universität Wien, Austria) for recording electrospray ionization mass spectra and Dr. G. Boschloo for interesting discussions. The authors gratefully acknowledge support from Swedish Energy Agency.

Supporting Information Available: Cyclic voltammograms, electrospray ionization mass spectra, and ¹H, ¹³C NMR and IR spectra of IILs. This material is available free of charge via the Internet at <http://pubs.acs.org>.

IC062244B